Science Press

Trans. Nonferrous Met. Soc. China 17(2007) s589−s593

Transactions of Nonferrous Metals Society of China

www.csu.edu.cn/ysxb/

Debinding and sintering of warm compacted and binder-treated complex iron-base part

NGAI Tungwai Leo(倪东惠), ZHOU Shui-bo(周水波), XIAO Zhi-yu(肖志瑜), LI Yuan-yuan(李元元)

Guangdong Key Laboratory for Advanced Metallic Materials Fabrication and Forming,
School of Mechanical Engineering, South China University of Technology, Guangzhou 510640, China

Received 15 July 2007; accepted 10 September 2007

Abstract: Regular elemental powders were used in warm flow compaction instead of the expensive micron-sized powders to fabricate cross-shaped parts. Debinding behaviors, sintering properties and shape consistency of the sintered parts were studied. Binder removal was accomplished by heating green compacts at intermediate temperatures with optimal heating rates until the debinding temperature was reached. Results show that by controlling debinding process, complex parts with good shape consistence can be obtained by warm compaction of binder-treated powder. Fine and shiny surface was obtained and no surface defect can be observed for sintered parts debinded at 2 ℃/min, while defect can be observed in sintered parts debinded at 4 ℃/min.

Key words: binder-treated powder; warm compaction; debinding; complex powder metallurgy part

1 Introduction

Powder metallurgy (PM) process is an economical net-shape manufacturing technique. Unfortunately, conventional PM is not capable of producing complex parts with aspects lateral to pressing direction[1]. However, a recently developed warm flow compaction (WFC) technique[2] can overcome this problem by increasing the flowability of the mixed powder and gives the powder the capability to flow around corners without forming shear cracks in the green during compaction. WFC uses higher binder content than conventional die pressing but considerably lower than metal injection molding. The flowability of the WFC powder was enhanced by blending in an appropriate ratio of fine powder fraction to lubricating binders. The highly admixed binder content transformed the powder-binder blend into a highly filled liquid forms during heating[3]. Optimal binder should have a favorable rheological property and is capable of undergoing complete transformation into small and non-toxic volatile compounds during the debinding process. Basic debinding process includes thermal debinding, solvent debinding and wick debinding[4]. Proper removal of organic binder is vital in obtaining sintered part with good mechanical property and shape consistence[5]. Thus, understanding the binder degradation kinetics and whether it interacts with inorganic powders are key issues to avoid inappropriate debinding operation[6−8]. In thermal debinding process, binder removal was accomplished by heating green compact at intermediate temperature with optimal heating rate to avoid rapid phase transformation of the binder. Sudden accumulation of the evolving gases in the compact should be avoided since it will generate high pressure buildup, which may lead to defects[8−10] such as blistering, warping, and skin exfoliation in the sintered product.

In this study, regular elemental powders were used, instead of the expensive micron-sized powders that used in WFC, to fabricate cross-shaped parts. Debinding kinetics and sintered properties were also studied.

2 Experimental

2.1 Materials and sample preparation

Foundation item: Projects(50574041, 50325516) supported by the National Natural Science Foundation of China; projects(2006Z1-D6081, 06105411) supported by Guangdong Science and Technology; project (NCET-05-0739) supported by NCET

Corresponding author: NGAI Tung-wai Leo; Tel: +86-20-87112948-205; E-mail: dhni@scut.edu.cn

High purity water atomized iron powder with an average particle size of 75 μm was used as base material. Ni powder (＜75 μm), Mo powder (＜75 μm) and graphite powder (＜75 μm) were used as alloying elements. Compositions(mass fraction) of the mixed powder were 96.5% Fe, 2.0% Ni, 0.5% Mo and 1.0% C.

After pre-mixed in a V-type mixing machine for 1 h, the mixed powder was then wet mixed with 3% and 6% of binder, which consists of waxes and polymers. The waxes (paraffin wax and carnauba wax) provide lubrication and viscosity during warm compaction, while the polymers bind the powder together. After drying, the mixture was ground and screen to be less than 150 μm. The pre-heated mix powder was then pressed in a heated steel mold, with a cross-shaped cavity at 163 ℃. Standard tensile test specimens (GB 7963—1987) were also prepared to measure the tensile property. Compacting pressure was 600 MPa and pressing speed was 250 mm/min. Lubrication oil was brushed on the inner die wall for lubrication.

Green compacts were debinded at 500 ℃ for 1 h, using heating rates of 2 and 4 ℃/min, in the pre-heating zone of a pusher type furnace under the reduced H_2-N_2 atmosphere. After debinding, the samples were sintered at 1 120 and 1 300 ℃ for 1 h, then subsequently cooled to room temperature.

2.2 Thermogravimetric measurement

Thermogravimetric (TG) measurements were carried out on a Netszh STA449 Jupiter Simultaneous Thermal Analyzer to provide thermal debinding information and the possible effect of inorganic powders on the binder decomposition. About 8 mg of binder and 45 mg of mixed powder+6% binder were heated from 313 to 823 K under N_2 atmosphere. Heating rates of 2, 5, 8 and 11 K/min were used.

2.3 Properties measurements

Ultimate tensile strength, elongation, green and sintered densities were measured. Density was measured by Archimedes method. A computer controlled universal testing machine was used to measure the green strength, tensile strength and elongation. Dimensional change after sintering was measured by micrometer according to GB/T 5159—1985. Data reported in this study were the average of at least three separate measurements.

3 Results and discussion

3.1 Thermal debinding

As suggested by GERMAN[5], thermal debinding starts with the binder decomposition at the binder/gas interface, and the evolving gas diffuses or permeates to the surface through inter-particle voids. As debinding continues, the binder progressively retreats toward the center of the body. Thermal debinding process usually starts with the binder melting. According to WOODTHORPE et al[11], it can be divided into three phases: 1) initial phase, where pores start forming; 2) intermediate phase, where interconnected pores form; and 3) final phase, where all binder are eliminated. Fig.1(a) shows TG curves of binder. It can be seen that the binder elimination starts gently at approximately 180 ℃ then the elimination rate increases rapidly at about 350 ℃. Not considering the melting stage (before 180 ℃), this debinding process mainly consists of two stages. First, low melting point waxes are eliminated, at which pores and interconnected pores form (stage 1, 180−350 ℃) then the elimination of the polymeroccurs, at which all binder are eliminated (stage 2, 350−490 ℃). Fig 1(b) shows TG curves of the mixed powder+6% binder. Although not as clear as those in Fig.1(a), the two debinding stages can be distinguished within the same temperature range.

TG curves of the mixed powder+binder show a gradual mass loss during the whole debinding process. Binder elimination starts at about 180 ℃ and elimination rate becomes significant at about 250 ℃. It is at this intermediate temperature that interconnected

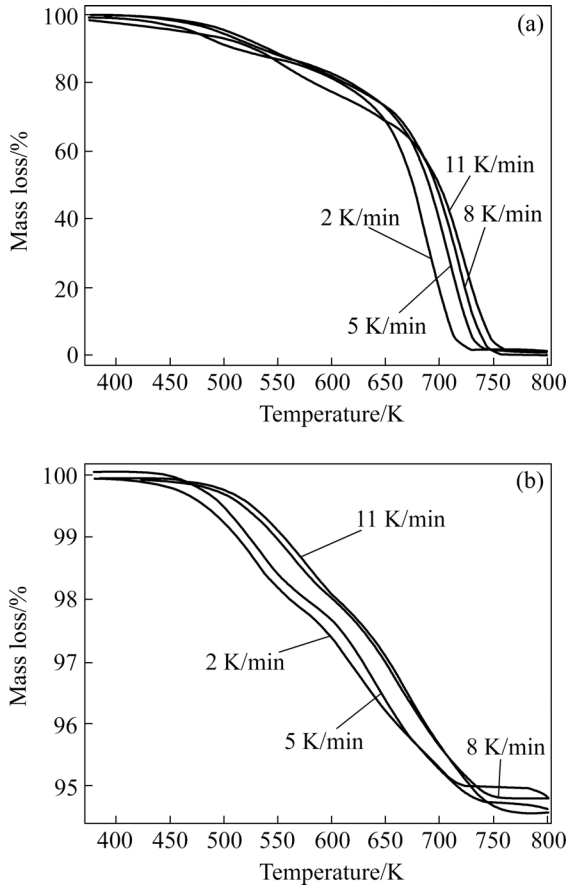

Fig.1 TG curves at different heating rates: (a) Binder only; (b) Mixed powder with 6% binder

pores should be developed to make room for vapor escaping and thus avoid rapid pressure buildup in the part; therefore reasonable slow binder elimination rate is preferred. Fig.1(b) shows that at low heating rates of 2 and 5 K/min, the elimination rate is only half of that of the higher heating rates. Thus 2 and 4 K/min are chosen as the heating rates and 773 K is selected as debinding temperature for debinding in the part preparation.

The rate constants for each stage were calculated from TG data using Eqn.(1)[12]:

$$k_{\mathrm{d}} = \frac{\Delta m}{\Delta t(m - m_{\mathrm{res}})} \tag{1}$$

where m is instantaneous mass, Δm is mass change during time Δt and m_{res} is residual mass at the end of the experiment. Rate constants obtained from each experiment are fitted to the Arrhenius expression[13]:

$$\ln k_{\mathrm{d}} = \ln A - \frac{E_{\mathrm{a}}}{RT} \tag{2}$$

where R is gas constant and T is absolute temperature. The pre-exponential factors A, and the activation energy, E_{a}, can be obtained from the slopes and intercepts from the linear fits to each of the TG experiments. The fittings can be divided into two regions that correspond to the two stages of the debinding process demonstrated in Fig.1. Figs.2 and 3 show the Arrhenius plots for samples of binder only and for powder+6% binder, respectively.

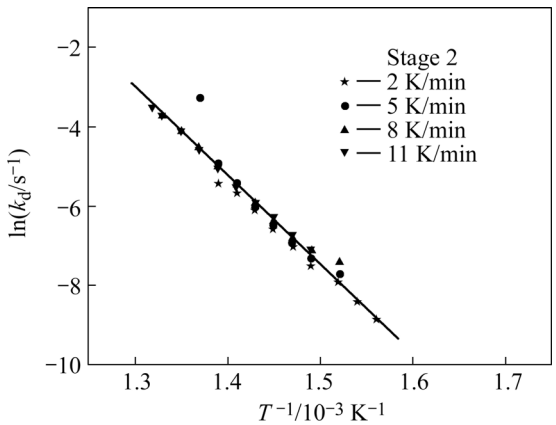

Fig.2 Arrhenius plot for binder only (stage 2)

Table 1 lists the calculated activation energy at different stages. The activation energy of thermal decomposition for pure binder is higher than that of powder+binder. The reason for this is not well known, but it is believed that the large surface area of the powder particles catalyze the binder decomposition in some complex manner[14−15].

Table 1 E_{a} calculated from TG experiments

Sample	Stage	E_{a}/(kJ·mol^{-1})
Binder only	2	180.9±3.5
Mixed powder with 6% binder	1	42.6±3.2
	2	75.1±4.9

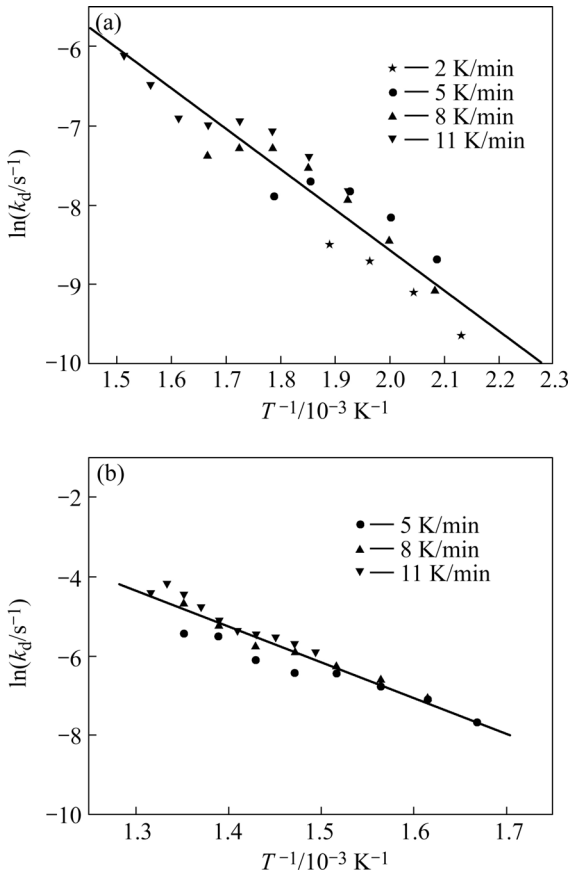

Fig.3 Arrhenius plots for powder + 6% binder: (a) stage 1; (b) stage 2

3.2 Properties of sintered part

As shown in Fig.4(a), sintered cross-shaped part is successfully prepared by binder-treated warm compaction, using a debinding rate of 2 ℃/min. Fine and shiny surface is obtained and no defect can be observed. While, defect such as cracks and surface pores can be observed for sintered parts debinded at 4 K/min, as shown in Fig.4(b). Experimental results show that heating rate of 2 K/min is good for debinding samples containing both 3% and 6% binder.

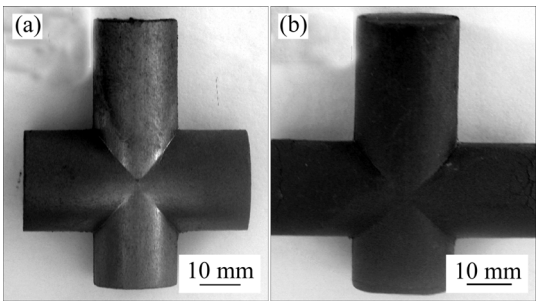

Fig.4 Photographs of sintered parts: (a) Debinded at 2 K/min; (b) Debinded at 4 K/min

Table 2 Densities and shrinkages of green and sintered parts debinded at 2 K/min

w(binder)/%	Green density/ ($g \cdot cm^{-3}$)	Sinter temperature/ ℃	Sintered density/ ($g \cdot cm^{-3}$)	Sinter shrinkage axial length/%	Sinter shrinkage axial diameter/%	Sinter shrinkage lateral length/%	Sinter shrinkage lateral diameter/%
3	5.952	1 120	6.339	−2.80	−0.19	−2.60	−0.26
		1 300	6.590	−2.80	−0.20	−2.50	−0.30
6	5.971	1 120	6.381	−4.87	−0.22	−5.71	−0.28
		1 300	6.720	−5.83	−0.27	−6.10	−0.31

Table 3 Property of tensile specimen

w(binder)/%	Green density/ ($g \cdot cm^{-3}$)	Green strength/ MPa	Sinter density/ ($g \cdot cm^{-3}$)	Tensile strength/ MPa	Elongation/%
3	6.456	31.7	6.920	514.0	5.9
6	6.477	30.7	7.490	430.8	2.6

Green density, sintered density, lateral and axial dimensional changes after sintering are listed in Table 2. For samples containing 3% binder, the green part has a density of 5.95 g/cm^3 and the part sintered at 1 300 ℃ has 6.59 g/cm^3. Compared with samples containing 3% binder, samples containing 6% binder have higher sintered density. The reason is probably that there is the better distribution of the alloying elements caused by the better fluidity of the powder mixture.

From Table 2, it can also be seen that consistent dimensional change is maintained for samples prepared by using 3% binder. All samples show negative dimensional change, which will increase the overall density of the part. This shrinkage effect can be compensated by adding proper amount of Cu, which gives positive dimensional change after sintering.

The benefit of using high binder concentration is that the powder has better flowability and thus better complex shape forming ability, but significant dimensional change will be introduced (as shown in Table 2) and debinding process becomes more difficult, especially for high green density parts. The high green density hinders the elimination of the evolving gases during debinding and causes various kinds of defects in the sintered sample.

Density and mechanical property of the tensile test specimen debinded at 2 K/min and sintered at 1 300 ℃ are listed in Table 3. Fine and shiny surface is obtained and no surface defect can be observed for sintered tensile specimen prepared by using 3% binder, while surface pores can be observed for sintered tensile specimen prepared by using 6% binder. This implies that heating rate of 2 K/min is not suitable for debinding compacts with high green density (approximately 6.46 g/cm^3 in this case), although it is good for debinding the cross-shaped part, which has a lower green density of approximately 5.96 g/cm^3. As shown in Table 3, due to the presence of pores, samples prepared by using 6% binder have lower tensile strength although it has higher sintered density.

4 Conclusions

1) Lower activation energy is needed for thermal debinding of the binder in the presence of the inorganic powders. 2 and 4 K/min are chosen as the heating rates and 500 ℃ is selected as debinding temperature for the debinding process.

2) Cross-shaped parts are prepared by binder-treated warm compaction method. Fine and shiny surface is obtained and no surface defect can be observed for sintered parts debinded at 2 K/min, while defect can be observed in sintered parts debinded at 4 K/min.

3) Tensile specimen prepared by using 3% binder and sintered at 1 300 ℃ has a density of 6.92 g/cm^3, tensile strength of 514 MPa and elongation of 5.9%.

References

[1] BEISS P. Competitive advantages by near-net-shape manufacturing[M]. KUNZE H D, Frankfurt: DGM Informationsgesellschaft, 1997: 189−209.

[2] VELTL G, PETZOLDT F. New developments in warm compaction[C]//Proceedings of European Conference on Advances in Structural PM Component Production '97. München, 1997: 36−43.

[3] VELTL G., OPPERT A, PETZOLDT F. Warm flow compaction fosters more complex PM parts[J]. MPR, 2001, 56(2): 26−28.

[4] GERMAN R M. Theory of thermal debinding[J]. Int J Powder Metall, 1987, 72: 237−245.

[5] GERMAN R M. Powder injection molding[M]. NJ: Metal Powder Industries Federation, 1990: 321−46.

[6] LOMBARDO S J, FENG Z C. Analytic method for the minimum time for binder removal from three-dimensional porous green bodies[J]. J Mat Res, 2003, 18: 2717−2723.

[7] LAM Y C, YING S, LAM K H, MA J, YU S C M, TAM K C.

Numerical and experimental investigation of thermal debinding[J]. Powder Metallurgy, 2002, 45(3): 233−236.

[8] SONG J H, EVANS J R G, EDIRINGHE M J, TWIZELL E H. Determination of gas transport coefficients in ceramic bodies during thermolysis of organic additives[J]. Int Materials Reviews, 1996, 41: 116−128.

[9] STANGLE G C, AKSAY I A. Simultaneous momentum, heat, and mass transfer with chemical reaction in a disordered porous medium: Application to binder removal from a ceramic green body[J]. Chem Eng Sci, 1990, 45: 1719−1731.

[10] ZHOU J , HUANG B, ZHANG C, LIU Y. Thermal debinding dynamics of novel binder system[J]. Trans Nonferrous Met Soc China, 2001 11(4): 517−520.

[11] WOODTHORPE J, EDIRISINGHE M J, EVANS J R G. Properties of ceramic injection moulding formulations (Ⅲ)—polymer removal[J]. J Mater Sci, 1989, 24: 1038−1048.

[12] JEE C S Y, GUO Z X, STOLIAROV S I, NYDEN M R. Experimental and molecular dynamics studies of the thermal decomposition of a polyisobutylene binder[J]. Acta Materialia, 2006, 54: 4803−4813.

[13] SAWAGUCHI T, TAKESUE T, IKEMURA T, SENO M. Thermal degradation of polymers in the melt. I: Characterization of volatile oligomers formed by thermal degradation of polyisobutylene[J]. Macromol Chem Phys, 1995, 196: 4139−4157.

[14] ZHANG L, ZHOU K, LI Z, ZHANG X. Degradation and the kinetics of binder removal[J]. Metal Powder Report, 2006, 61(11): 28−33.

[15] HRDINA K E, HALLORAN J W, OLIVEIRA A, KAVIANI M. Chemistry of removal of ethylene vinyl acetate binders[J]. J Mat Sci, 1998, 33: 2795−2803.

(Edited by CHEN Can-hua)